VNU Journal of Science: Mathematics – Physics, Vol. 38, No. 1 (2022) 111-118

VNU Journal of Science: Mathematics - Physics

Journal homepage: https://js.vnu.edu.vn/MaP

Original Article

Fabrication and Characteristics of Silica Nanoparticle Monolayer Assembled by Spin Coating

Nguyen Thi Thanh Lan, Chu Manh Hoang*

International Training Institute for Materials Science, Hanoi University of Science and Technology, No. 1, Dai Co Viet, Hai Ba Trung, Hanoi, Vietnam

Received 26 August 2020
Revised 6 September 2021; Accepted 15 September 2021

Abstract: In this paper, we report on a process for fabricating silica nanoparticle monolayer based on chemical synthesis and spin-coating. Spherical silica nanoparticles were synthesized by Stöber method using tetraethylorthosilicate as precursor. Close-packed silica nanoparticle monolayer was realized by optimizing the speed of spin-coating. Based on analyzing field emission scanning electron microscope (FE-SEM) images, the average diameter of silica spheres was determined and found of about 196 nm, with a standard deviation approximately ± 40 nm. The reflectance for the silicon substrate with spherical silica nanoparticle monolayers has been experimentally investigated at various spin-coating speeds. The experimental results are compared to those obtained from simulation data. The obtained results are useful for developing substrates having nanostructures for various applications in photonics and plasmonics.

Keywords: Silica nanoparticles, Stöber method, spin coating, self-assembled monolayer.

1. Introduction

Ordered nanostructures are interested for various applications, especially for enhancing the absorption of incident radiation in solar cell and in surface enhanced Raman scattering [1-5]. To prepare nanostructures, advanced fabrication methods have been used such as e-beam lithography, focus ion beam [4-9]. However, these methods are high-cost manufacturing technologies but with low throughput. Recently, innovation fabrication methods have been interested to develop for reducing the cost of production and increasing the accessibility of researchers. The most common method is colloidal lithography [5, 10-12]. In this method, an order monolayer of spherical nanoparticles is used as a mask

* Corresponding author.
E-mail address: hoangcm@itims.edu.vn

https//doi.org/10.25073/2588-1124/vnumap.4599

layer for patterning nanostructures. Spherical nanoparticles are usually formed in silica or polystyrene [10-13]. To fabricate spherical silica nanoparticles, the Stöber method is often used [14-16]. In principle, the Stöber method is a synthesis method in hydroxide medium. The formation of silica nanoparticles depends on various parameters such as concentration of precursors, NH_3, H_2O, TEOS, temperature, etc. There are various approaches for forming monolayers of spherical nanoparticles, for example, single-step freeze-drying coating, template-assisted self-assembly, direct assembly at the air–water interface, etc. [13, 17-22]. In [23], the monolayer of 284 nm polystyrene spheres is formed by the spin-coating method. The formation of spin-coating monolayer depends on many factors, such as spin speeds, spinning steps, spinning time, solution quantity, relative humidity, and size of nanoparticle. The recent effort in extending the 50 nm silica nanoparticle monolayer region is also developed by inclining substrate using drop coating and infrared irradiation [14]. When the size of nanoparticles decreases, it is not easy to form monolayers. Furthermore, fabrication of monolayers based on the spin-coating method for the small size silica nanoparticles has not been much studied.

In this work, we report on a process from the synthesis to the formation of the close-packaged monolayer of spherical silica nanoparticles. The size of fabricated silica nanoparticles and close-packaged monolayer were investigated by analyzing microimages obtained from a field emission scanning electron microscope (FE-SEM) Hitachi's S-4800. We also present the results of reflectance measurement of silica nanoparticle monolayers on silicon substrate. The experimental measurement results have been compared to those obtained from simulation data.

2. Experiments

2.1. Preparation of Silica Nanoparticle

Spherical silica nanoparticles were synthesized by Stöber method, using tetraethylorthosilicate (TEOS) as the precursor; ethanol solvent, water and ammonia as the agent and catalyst for hydrolysis reaction [15, 16]. The concentration and volume of the solutions are as follows: C_2H_5OH (50 ml), NH_3 2M (7.8 ml), TEOS 0.3M (5.34 ml). With the ratio of catalyst as above specified, the concentration of H_2O in ammonia solution is determined at about 5M. In this synthesis process, water is a hydrolyzing agent, transforming ethoxy groups to silanol groups, which are then condensed to form siloxane bridges by water or alcohol elimination. The hydrolysis reaction is written as follows:

$$\equiv \mathrm{Si} - \mathrm{OR} + \mathrm{H_2O} \rightarrow \equiv \mathrm{Si} - \mathrm{OH} + \mathrm{ROH} \quad (1)$$

The water condensation to form siloxane bridges is described by

$$\equiv \mathrm{Si} - \mathrm{OH} + \mathrm{HO} - \mathrm{Si} \equiv \rightarrow \equiv \mathrm{Si} - \mathrm{O} - \mathrm{Si} \equiv + \mathrm{H_2O} \quad (2)$$

The water is present in ammonia solution with relatively large amount, therefore, it does not supply further in the process, and the water concentration is adjusted according to the catalyst concentration.

The process for synthesizing spherical silica nanoparticles is shown in Fig. 1, slowly adding solution 1 containing the mixture of TEOS and C_2H_5OH (flask1) to flask 2 containing C_2H_5OH and NH_3 solution. The purpose of diluting the precursor and catalyst into the alcohol solvent is to make the feed rate of reactant more uniform and easily controlled. The final solution is magnetically stirred at room temperature for 3 h. During this period, hydrolysis and condensation reactions occur and the clear solution is gradually turned into milky white, indicating the formation of silica nanoparticles. The flask is left after reaction at room temperature for 24 h, and then silica nanoparticles are centrifuged and washed with ethanol repeatedly until pH $\approx$ 7. The silica nanoparticles are dispersed in ethanol and stored at low temperature.

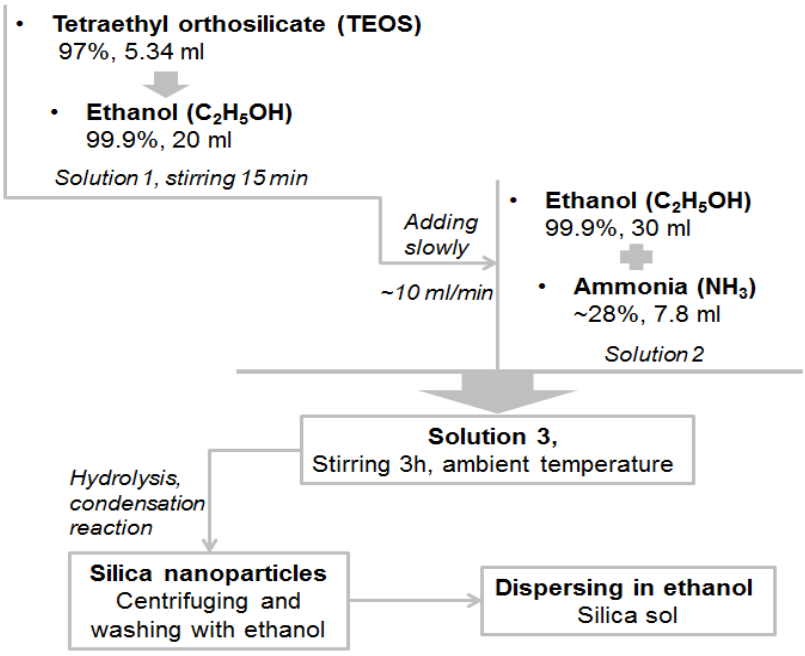

Figure 1. Synthesis process of spherical silica nanoparticles.

2.2. Silica Nanoparticle Monolayer Assembled by Spin-coating

Before coating, the n-type Si wafer of 1×1 cm^2 in size is cleaned by ultrasonic vibration in acetone, ethanol, deionized water for 15 min. Wet treatment to increase adhesion with solution and silica nanoparticles is performed by soaking the Si wafer in piranha solution (the volume ratio H_2SO_4 (98%):H_2O_2 (35 %) = 3:1) for 18 h at room temperature and rinsing with deionized water. Then, the wafer is treated with RCA-1 solution (the volume ratio NH_4OH (30 %):H_2O_2:H_2O = 1:1:5) at 75 ^oC for 30 min, rinsed many times with deionized water and centrifugal dry before use. The surface of the wafer after wet treatment in the above solutions forms a hydrophilic silanol group (Si-OH) and effectively removes organic and inorganic contaminants. The wet-treated wafer may be stored in deionized water and used for one week.

Dimethyl formaldehyde solvent (DMF) is added into the initial silica sol to reduce the surface tension of the sol, increase capillary force for keeping particles arranged closely together, the volume ratio DMF:EtOH = 1:1 (silica concentration ~ 5 wt%), and using ultrasonic vibration to disperse sol again. A small amount of sol, which is sufficient to spread over the entire surface (7÷10 μL), is dropped onto the Si wafer, and performing one-step spin-coating under ambient temperature condition of 25 °C and relative humidity of 65% for 150 s.

3. Results and Discussion

3.1. Size Distribution of Silica Nanoparticles

The silica nanoparticle size distribution can be determined by either dynamic light scattering (DSL) [24], or estimating from SEM/TEM image data, using image analysis software- Image [22]. Fabricated silica nanoparticles have uniform round shape without particle agglomeration, Figure 2a shows an

assembled silica nanoparticle monolayer array. Figure 2b shows the size distribution chart of fabricated silica nanoparticle array on silicon substrate. The average diameter of silica spheres is 196 nm with a standard deviation approximately ± 40 nm. To obtain more uniform nanoparticles, the following experiment parameters are necessary: The time of initial seed formation should be reduced and seed formation should be prevented at the later stage by increasing the temperature in the first stage Reducing the concentration of the catalyst; Increasing the stirring time; Ensuring that the reaction takes place almost completely before being in the static state. In Ref [25], five main parameters have been considered to influence the size and size distribution of the silica nanoparticles including concentration of TEOS, NH_3, and H_2O, type of used alcohol solvent, and reaction temperature. The ratio R (= [H_2O]/[TEOS]), the feed rate of reactant, has also been investigated such as another influencing parameter [26]. The results from studies using ethanol solvent suggested that the appropriate concentrations for synthesis of silica nanoparticles of a few hundred nanometers size are about 0.2÷0.4 M, 1÷10 M and 2÷15 M for TEOS, NH_3 and H_2O, respectively [27, 28].

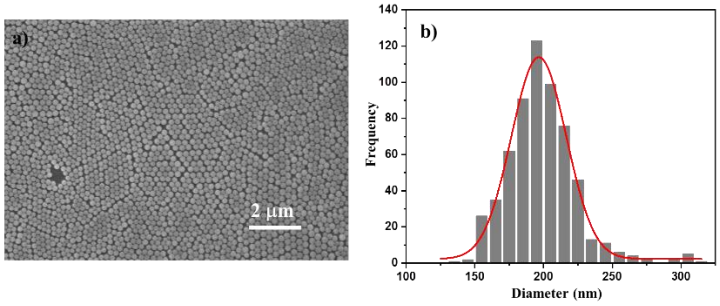

Figure 2. a) FESEM image and b) size distribution chart of fabricated silica nanoparticle array on silicon substrate.

3.2. Effect of Spin-coating Speed

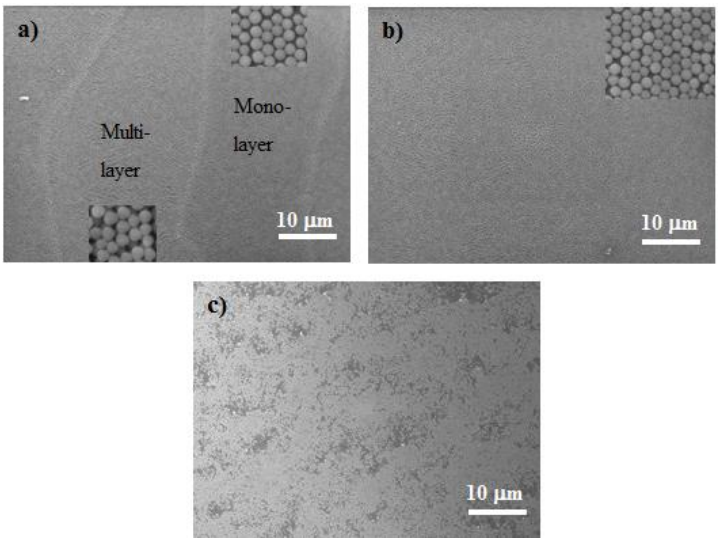

Figure 3. FESEM images of spherical silica nanoparticles on silicon substrate spin-coated a t a) 1500 rpm, b) 2000 rpm, and c) 3000 rpm.

Figure 3 shows the results of assembling silica nanoparticle monolayer at different spin-coating speeds. Monolayer with hexagonal close-packed type of silica nanoparticle array is evenly observed

across the whole wafer with an area of 1 cm^2, corresponding to the spin-coating speed at 2000 rpm (Figure 3b). The multilayer or mixture of monolayer and multilayer is formed at smaller speeds (1500 rpm, Figure 3a), and at higher speeds (3000 rpm, Figure 3c), it only obtains non-uniform distributed monolayer. The monolayer formation is governed by centrifugal, hydrophilic and capillary forces [23, 29, 30], which are influenced by spin speed, sol characteristics and ambient conditions. The centrifugal force helps the sol to spread evenly on silicon wafer, while the capillary and hydrophilic forces tend to keep the particles close together. So with the above fabricated sol and ambient conditions, the optimal coating speed to obtain a close-packed monolayer is around 2000 rpm.

3.3. Optical Reflectance Characterization of Silica Nanoparticle Monolayer on Silicon Wafer

The silica nanoparticles have sub-wavelength size, and they are not scattered elements due to their good transmittance property. Therefore, there is almost no high-order diffraction in different directions, and the silica nanoparticle layer is considered to be an effective layer having a thickness equal to the average height of silica nanoparticles and effective refractive index to be n_{eff}. When the light is irradiated onto Si substrate containing silica nanoparticles, only specular reflection occurs. It is easy to obtain the reflection spectrum of the silica nanoparticle sample with a common spectrometer without the use of integrating sphere. The measurement was performed on ultraviolet-visible-near-infrared (UV-Vis-NIR) spectrophotometer (Jasco V770) with an incident angle of ~ 5°, beam size ~ 7 mm. The result in Figure 4a is the reflection spectra of Si substrate covered with silica nanoparticles at spin-coating speeds of 1500 rpm, 1800 rpm and 2000 rpm.

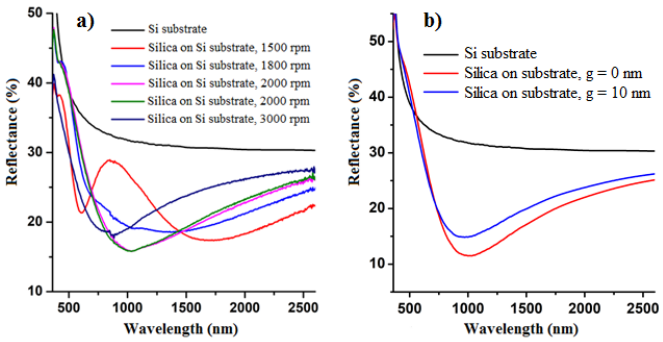

Figure 4. (a) Reflectance measured for the Si substrate with spherical silica nanoparticle layers at various spin-coating speeds and (b) reflectance spectra calculated with assuming $n_{SiO2} = 1.48$.

The reflectance spectra of two samples of monolayer assembled at the optimized spin-coating speed of 2000 rpm are also shown in Figure 4a. These two samples have the same curves of reflectance spectra. In this study, we have also investigated the reflectance spectra of the samples similar to Figure 4a. The geometrical parameters of the substrate are taken from the FE-SEM images, in which the size of spherical silica nanoparticle is 196 nm, the refractive index of silica is 1.48. The results of theoretical calculations are shown in Figure 4b, for the bare silicon substrate and silicon substrate having silica nanoparticle monolayer with the gap among nanoparticles g = 0 nm and g = 10 nm. Here, the theoretical reflectance curves are calculated by finite element method using Wave Optics Module in Comsol software, solved for the full field. The optical parameters of silicon in the 0.25-1.4 μm and 1.4-2.6 μm wavelength ranges are taken from Refs. [31] and [32], respectively, and assumed that the imaging (κ) and real (n) parts of complex refractive index of nanosilica are κ = 0, n = 1.48 in the investigated spectral range, respectively. Thus, the experimental spectral profiles are similar to those obtained from theoretical calculations. This also proves that the monolayer of nanoparticles is uniform on the whole

silicon wafer. In addition, the refractive index of nanosilica and effective layer are smaller than that of bare silicon substrate, the reflectivity of the Si substrate covered with silica nanospheres is lower than that of Si substrate. When the phase deviation is equal to $(2k+1)\pi$, the interference between the reflected waves from the upper and lower surfaces of the effective monolayer has destructive tendency that leads to minimum reflection, corresponding to the condition $d=(2k+1)\lambda/4n_{eff}$. The sample coated with a lower spin-coating speed (namely 1500 rpm) results in a multi-layered array or a mixture of single-layer and multi-layer. In this case, the reflectance minimum moves toward the long wavelength and the second minimum appears in the visible region due to the optical thickness $n_{eff}.d$ increases. As the spin-coating rate increases, leading to forming a non-close-packed monolayer, the effective refractive index n_{eff} decreases and the absolute difference $\left|\sqrt{n_{Si}}-n_{eff}\right|$ increases, so the minimum of reflectance is blue shifted and tends to be shallower (Fig. 4a). Thus, the silicon substrates with close-packed monolayer (there is no clear reflective color) can be determined based on uniform observation and reflectance spectrometry.

4. Conclusion

We have presented the results of fabricating close-packed silica nanoparticle monolayer based on chemical synthesis using Stöber method and optimization of spin-coating. Close-packed silica nanoparticle monolayer is realized by optimizing the speed of spin-coating. By analyzing field emission scanning electron microscope images, the average diameter of silica spheres has been evaluated to be of 196 nm with a standard deviation approximately ± 40 nm. The reflectance for the silicon substrate with self-assembled spherical silica nanoparticle monolayers has been experimentally investigated at various spin-coating speeds. The experimental results are in good agreement with those obtained from simulation data. The close-packed silica nanoparticle monolayers are successfully assembled on the silicon wafer. This is useful for further design and fabrication of photonic and plasmonic nanostructures.

Acknowledgment

This work is financially supported by the Vietnam Ministry of Education and Training, Project number B2020-BKA-23-CTVL.

References

[1] E. Garnett, P. Yang, Light Trapping in Silicon Nanowire Solar Cells, Nano Lett., Vol. 10, No. 3, 2010, pp. 1082-1087, https://doi.org/10.1021/nl100161z.

[2] P. R. Pudasaini, F. R. Zepeda, M. Sharma, D. Elam, A. Ponce, and A. A. Ayon, High Efficiency Hybrid Silicon Nanopillar–polymer Solar Cells, ACS Appl. Mater. Interfaces, Vol. 5, No. 19, 2013, pp. 9620-9627, https://doi.org/10.1021/am402598j.

[3] G. X. Li, Z. L. Wang, S. M. Chen, K. W. Cheah, Narrowband Plasmonic Excitation on Gold Hole-array Nanostructures Observed Using Spectroscopic Ellipsometer, Opt. Express, Vol. 19, No. 7, 2011, pp. 6348-6353, https://doi.org/10.1364/OE.19.006348.

[4] G. F. Walsh, L. D. Negro, Enhanced Second Harmonic Generation by Photonic–plasmonic Fano-type Coupling in Nanoplasmonic Arrays, Nano Lett., Vol. 13, No. 7, 2013, pp. 3111-3117, https://doi.org/10.1021/nl401037n.

[5] J. Jiang, X. Wang, S. Li, F. Ding, N. Li, S. Meng, R. Li, J. Qi, Q. Liu, G. L. Liu, Plasmonic Nano-arrays for Ultrasensitive Bio-sensing, Nanophotonics, Vol. 7, No. 9, 2018, pp. 1517-1531, https://doi.org/10.1515/nanoph-2018-0023.

[6] Y. Kanamori, K. Hane, Broadband Antireflection Subwavelength Gratings for Polymethyl Methacrylate Fabricated with Molding Technique, Opt. Rev., Vol. 9, No. 5, 2002, pp. 183-185, https://doi.org/10.1007/s10043-002-0183-0.

[7] Y. Kanamori, H. Katsube, T. Furuta, S. Hasegawa, K. Hane, Design and Fabrication of Structural Color Filters with Polymer-based Guided-mode Resonant Gratings by Nanoimprint Lithography, Jpn. J. Appl. Phys., Vol. 48, No. 6, 2009, pp. 06FH04, https://doi.org/10.1143/JJAP.48.06FH04.

[8] X. Q. Zhang, W. J. Salcedo, M. M. Rahmana, A. G. Brolo, Surface-enhanced Raman Scattering from Bowtie Nanoaperture Arrays, Surf. Sci., Vol. 676, 2018, pp. 39–45, https://doi.org/10.1016/j.susc.2018.02.003.

[9] G. A. Baker, D. S. Moore, Progress in Plasmonic Engineering of Surface-enhanced Raman-scattering Substrates Toward Ultra-trace Analysis, Anal. Bioanal. Chem., Vol. 382, 2005, pp. 1751-1770, https://doi.org/10.1007/s00216-005-3353-7.

[10] D. G. Choi, H. K. Yu, S. G. Jang, S. M. Yang, Colloidal Lithographic Nanopatterning via Reactive Ion Etching, J. Am. Chem. Soc., Vol. 126, No. 22, 2004, pp. 7019-7025, https://doi.org/10.1021/ja0319083.

[11] P. Hanarp, D. S. Sutherland, J. Gold, B. Kasemo, Control of Nanoparticle Film Structure for Colloidal Lithography, Colloids Surf. A: Physicochem. Eng. Aspects, Vol. 214, No. 1-3, 2003, pp. 23-36, https://doi.org/10.1016/S0927-7757(02)00367-9.

[12] X. Liu, W. Liu, B. Yang, Deep-elliptical-Silver-nanowell Arrays (d-EAgNWAs) Fabricated by Stretchable Imprinting Combining Colloidal Lithography: A Highly Sensitive Plasmonic Sensing Platform, Nano Res., Vol. 12, 2019, pp. 845–853, https://doi.org/10.1007/s12274-019-2302-2.

[13] C. Feng, H. W. Choi, Density-tunable Non-close-packed Monolayer of Silica Nanospheres Prepared by Single-step Freeze-drying, J. Vac. Sci. Technol. B, Vol. 32, No. 5, 2014, pp. 051805, https://doi.org/10.1116/1.4895037.

[14] N. V. Minh, N. T. Hue, N. T. H Lien, C. M. Hoang, Close-packed Monolayer Self-assembly of Silica Nanospheres Assisted by Infrared Irradiation, Electron. Mater. Lett., Vol. 14, 2018, pp. 64-69, https://doi.org/10.1007/s13391-017-6389-x.

[15] W. Stöber, A. Fink, E. Bohn, Controlled Growth of Monodisperse Silica Spheres in the Micron Size Range, J. Colloid Interface Sci., Vol. 26, No. 1, 1968, pp. 62–69, https://doi.org/10.1016/0021-9797(68)90272-5.

[16] T. H. L. Nghiem, T. N. Le, T. H. Do, T. T. Duong, V. Q. Hoa, D. H. N. Tran, Preparation and Characterization of Silica–Gold Core–shell Nanoparticles, J. Nanopart. Res., Vol. 15, 2013, pp. 2091, https://doi.org/10.1007/s11051-013-2091-6.

[17] Y. Yin, Y. Lu, B. Gates, Y. Xia, Template-assisted Self-assembly: A Practical Route to Complex Aggregates of Monodispersed Colloids with Well-defined Sizes, Shapes, and Structures, J. Am. Chem. Soc., Vol. 123, No. 36, 2001, pp. 8718-8729, https://doi.org/10.1021/ja011048v.

[18] N. Vogel, S. Goerres, K. Landfester, C. K. Weiss, A Convenient Method to Produce Close- and Non-close-packed Monolayers Using Direct Assembly at the Air–water Interface and Subsequent Plasma-Induced Size Reduction, Macromol. Chem. Phys., Vol. 212, No. 16, 2011, pp. 1719-1734, https://doi.org/10.1002/macp.201100187.

[19] M. Schmudde, C. Grunewald, C. Goroncy, C. N. Noufele, B. Stein, T. Risse, C. Graf, Controlling the Interaction and Non-close-packed Arrangement of Nanoparticles on Large Areas, ACS Nano, Vol. 10, No. 3, 2016, pp. 3525-3535, https://doi.org/10.1021/acsnano.5b07782.

[20] X. Yan, J. Yao, G. Lu, X. Li, J. Zhang, K. Han, B. Yang, Fabrication of Non-close-packed Arrays of Colloidal Spheres by Soft Lithography, J. Am. Chem. Soc., Vol. 127, No. 21, 2005, pp. 7688-7689, https://doi.org/10.1021/ja0428208.

[21] P. Jiang, T. Prasad, M. J. McFarland, V. L. Colvin, Two-dimensional Nonclose-packed Colloidal Crystals Formed by Spincoating, Appl. Phys. Lett., Vol. 89, 2006, pp. 11908, https://doi.org/10.1063/1.2218832.

[22] N. V. Minh, N. N. Son, N. T. H. Lien, C. M. Hoang, Non-close Packaged Monolayer of Silica Nanoparticles on Silicon Substrate Using HF Vapor Etching, Micro & Nano Letters, Vol. 12, No. 9, 2017, pp. 656-659, https://doi.org/10.1049/mnl.2016.0825.

[23] S. S. Shinde, S. Park, Oriented Colloidal-crystal Thin Films of Polystyrene Spheres via Spin Coating, J. Semicond., Vol. 36, No. 2, 2015, pp. 023001, https://doi.org/10.1088/1674-4926/36/2/023001.

[24] P. Kozma, B. Fodor, A. Deak, P. Petrik, Optical Models for the Characterization of Silica Nanosphere Monolayers Prepared by the Langmuir-Blodgett Method Using Ellipsometry in the Quasistatic Regime, Langmuir, Vol. 26, No. 20, 2010, pp. 16122–16128, https://doi.org/10.1021/la1028838.

[25] G. H. Bogush, M. A. Tracy, C. F. Zukoski, Preparation of Monodisperse Silica Particles: Control of Size and Mass Fraction, J. Non-Cryst. Solids, Vol. 104, No. 1, 1988, pp. 95-106, https://doi.org/10.1016/0022-3093(88)90187-1.

[26] S. K. Park, K. D. Kim, H. T. Kim, Preparation of Silica Nanoparticles: Determination of the Optimal Synthesis Conditions for Small and Uniform Particles, Colloids Surf. A: Physicochem. Eng. Aspects, Vol. 197, No. 1-3, 2002, pp. 7-17, https://doi.org/10.1016/S0927-7757(01)00683-5.

[27] W. Stober, A. Fink, E. Bohn, Controlled Growth of Monodisperse Silica Spheres in the Micron Size Range, J. Colloid Interface Sci., Vol. 26, 1968, pp. 62-69, https://doi.org/10.1016/0021-9797(68)90272-5.

[28] G. H. Bogush, C. F. Zukoski, Studies of the Kinetics of the Precipitation of Uniform Silica Particles through the Hydrolysis and Condensation of Silicon Alkoxides, J. Colloid Interface Sci., Vol. 142, No. 1, 1991, pp. 1-18, https://doi.org/10.1016/0021-9797(91)90029-8.

[29] T. Ogi, L. B. M. Lopez, F. Iskandar, K. Okuyama, Fabrication of a Large Area Monolayer of Silica Particles on a Sapphire Substrate by a Spin Coating Method, Colloids Surf. A: Physicochem. Eng. Aspects, Vol. 297, No. 1-3, 2007, pp. 71-78, https://doi.org/10.1016/j.colsurfa.2006.10.027.

[30] S. Khanna, P. Marathey, Utsav, H. Chaliyawala, N. Rajaram, D. Roy, I. Mukhopadhyay, Fabrication of Long-ranged Close-packed Monolayer of Silica Nanospheres by Spin Coating, Colloids Surf. A: Physicochem. Eng. Aspects, Vol. 553, 2018, pp. 520-527, https://doi.org/10.1016/j.colsurfa.2018.05.063.

[31] M. A. Green, Self-consistent Optical Parameters of Intrinsic Silicon at 300K Including Temperature Coefficients, Sol. Energ. Mat. Sol. Cells, Vol. 92, No. 11, 2008, pp. 1305-1310, https://doi.org/10.1016/j.solmat.2008.06.009.

[32] H. H. Li., Refractive Index of Silicon and Germanium and Its Wavelength and Temperature Derivatives, J. Phys. Chem. Ref. Data, Vol. 9, No. 3, 1993, pp. 561-658, https://doi.org/10.1063/1.555624.